THE SPACE SURVEILLANCE TELESCOPE: FOCUS AND ALIGNMENT OF A THREE MIRROR TELESCOPE

Deborah F. Woods
MIT Lincoln Laboratory

Ronak Shah
MIT Lincoln Laboratory

Julie Johnson
MIT Lincoln Laboratory

Alexander Szabo
MIT Lincoln Laboratory

Eric C. Pearce
MIT Lincoln Laboratory

Richard Lambour
MIT Lincoln Laboratory

Walter Faccenda
MIT Lincoln Laboratory

ABSTRACT

The Space Surveillance Telescope (SST) is a DARPA-funded technology initiative to dramatically increase sensitivity to microsatellites at the geosynchronous belt and to improve cataloging of the deep space resident space object (RSO) population. The SST achieves increased sensitivity to faint objects and rapid search capabilities by combining a large 3.5 m aperture Mersenne-Schmidt telescope design and a highly sensitive curved mosaic focal surface CCD camera. While the unique system design is advantageous for space surveillance capabilities, it presents a challenge to alignment due to an inherently small depth of focus and the additional degrees of freedom introduced with a powered tertiary mirror. This paper will provide a brief overview of the SST, discuss the methodology for achieving and maintaining focus and alignment of the system across a range of temperature and elevation conditions, and present recent results of the system alignment performance.

This work is sponsored by the Defense Advanced Research Projects Agency under Air Force Contract #FA8721-05-C-0002. Opinions, interpretations, conclusions and recommendations are those of the author and are not necessarily endorsed by the United States Government.

1. INTRODUCTION

The Space Surveillance Telescope (SST) is a DARPA sponsored technology developed by MIT Lincoln Laboratory to significantly enhance the nation's capabilities in space situational awareness. The SST's mission is to provide timely observations of satellites and space debris, particularly at the geosynchronous region located at approximately 36,000 km from the Earth's surface. The proliferation of microsatellites and space debris underscores the importance of building and maintaining accurate and complete cataloging of space objects. Current knowledge of the space environment is key to safeguarding vital space resources.

The SST features a 3.5 m primary mirror with an unconventional Mersenne-Schmidt design incorporating an advanced curved focal surface CCD. The telescope has an unusually short focal ratio, f/1.0, allowing for the combination of a highly agile mount with a wide field-of-view, 6 square degrees. L-3 Brashear designed the telescope structure and pointing system. The wide field-of-view, large aperture, and mount performance enable the system to scan the whole sky multiple times per night. The optical design achieves uniform illumination of the 12 CCD devices aligned to the curved Mersenne-Schmidt focal surface. Each CCD has 2048 by 4086 15 μm pixels.

The location on an 8000 ft peak in the White Sands Missile Range (WSMR) south of Socorro, NM, provides a dry environment with excellent seeing conditions. The optics developed by L-3 Brashear takes full advantage of the astronomical seeing conditions and pixel resolution.

The SST achieved first light in February 2011 and since then has conducted regular observations to test space surveillance functionality and performance. The telescope system is shown in Fig.1. The ability of the SST to achieve and maintain focus contributes to its overall system performance. The limiting magnitude varies with the focus performance because a blurry spot causes the signal to be smeared over more pixels, which decreases the signal-to-noise ratio for a given set of observing conditions. System models show that the limiting magnitude degrades as the spot size increases as shown in Fig. 2.

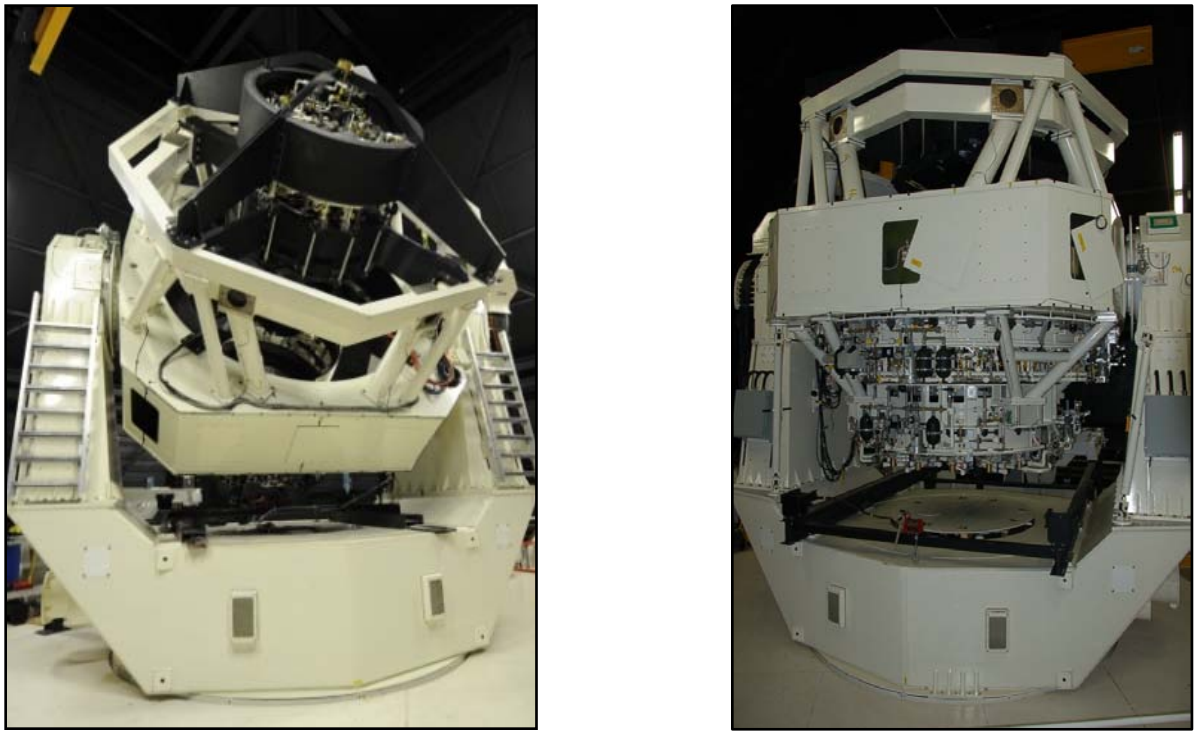

Figure 1: Two images of the Space Surveillance Telescope (SST). The telescope is a Mersenne-Schmidt system with powered primary, secondary, and tertiary mirrors. The compact layout achieved by the F/1.0 optics facilitates the mount gimbal's pointing performance.

One unique aspect of the SST system design is that there are no dedicated focus actuators. The hydraulic support system does the focusing and also provides solid body motion of the mirror. The support systems of the secondary and tertiary mirrors provide sufficient range of motion to maintain focus over all orientations and temperatures. Each mirror has nominally four degrees of freedom: translation along the optical axis ("piston"), rotation about the elevation axis ("tip"), rotation along the elevation axis ("tilt") and translation in the direction perpendicular to the elevation axis ("decenter"). The mirror motion is achieved using a large number of hydraulic powered actuators. In principle, we move the tertiary to achieve most of the aberration reduction. The secondary is used next, and mostly in piston to alleviate spherical aberration. The primary mirror serves as a reference surface and is assumed to be fixed. The focal surface of the camera is fixed with respect to the tertiary mirror cell.

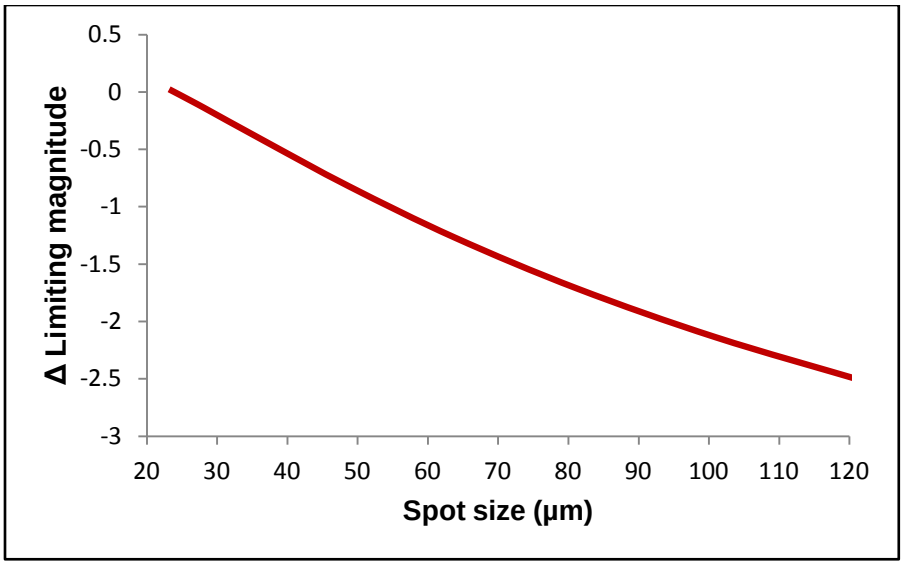

Figure 2: The predicted impact of spot size on the system performance in terms of limiting magnitude for a constant integration time and set of atmospheric conditions. The limiting magnitude degrades substantially as the spot size grows, smearing the signal over additional pixels and increasing the signal-to-noise ratio.

Focus and alignment of the SST is accomplished without a dedicated wavefront sensor or other permanent focusing instrumentation. Given the volumetric constraints of the narrow depth of focus and the need to have large amounts of the field of regard available for the primary mission, an alternative, image-based method was desired. We carry out system alignment based on estimation of the optical aberrations present in the system using defocused imagery. The DONUT program [1] provides the algorithms for measurement of optical aberrations from a single defocused star, which we adapt for use on the SST. We then consult our Zemax model of the as-built optical system to determine appropriate mirror position shifts that compensate or remove the measured aberrations.

In this paper we describe the method that we developed for the focus and alignment of the SST and present results of the system alignment performance. Section 2 contains an introduction to the measurement and representation of wavefront aberrations; Section 3 provides details on the focus and alignment method to achieve best focus at zenith pointing; Section 3.1 introduces operational focus considerations; Section 3.2 discusses adjustments to focus and alignment at different elevation angles, Section 3.3 describes the effects of temperature variation; Section 4 includes a summary and conclusion.

2. MEASUREMENT OF OPTICAL ABERRATIONS

The focus and alignment of the SST is accomplished through the estimation of optical aberrations using deliberately defocused star imagery. We use the DONUT algorithms by Tokovinin and Heathcote, which estimate the Zernike aberrations present in an optical system based on imaging of a single defocused star [1]. (A defocused stellar image is donut-shaped in a telescope with a central obscuration, hence the name of the algorithm.) The intensity distribution in an image relates to the local wavefront curvature through the irradiance transport equation [2]. The DONUT method reconstructs the wavefront shape from a defocused star using the Zernike polynomials. The Zernike polynomials provide a convenient representation of wavefront aberrations in an optical system because they form a complete basis that is orthogonal over the unit circle and have separable radial and angular contributions [3]. Fig. 3 show the wavefront aberrations in terms of the Zernike polynomials. In this paper we use the standard Noll convention for the ordering of the Zernike terms [4]. Additional detail on the application of the DONUT algorithms to the SST data will be provided in a forthcoming paper [5].

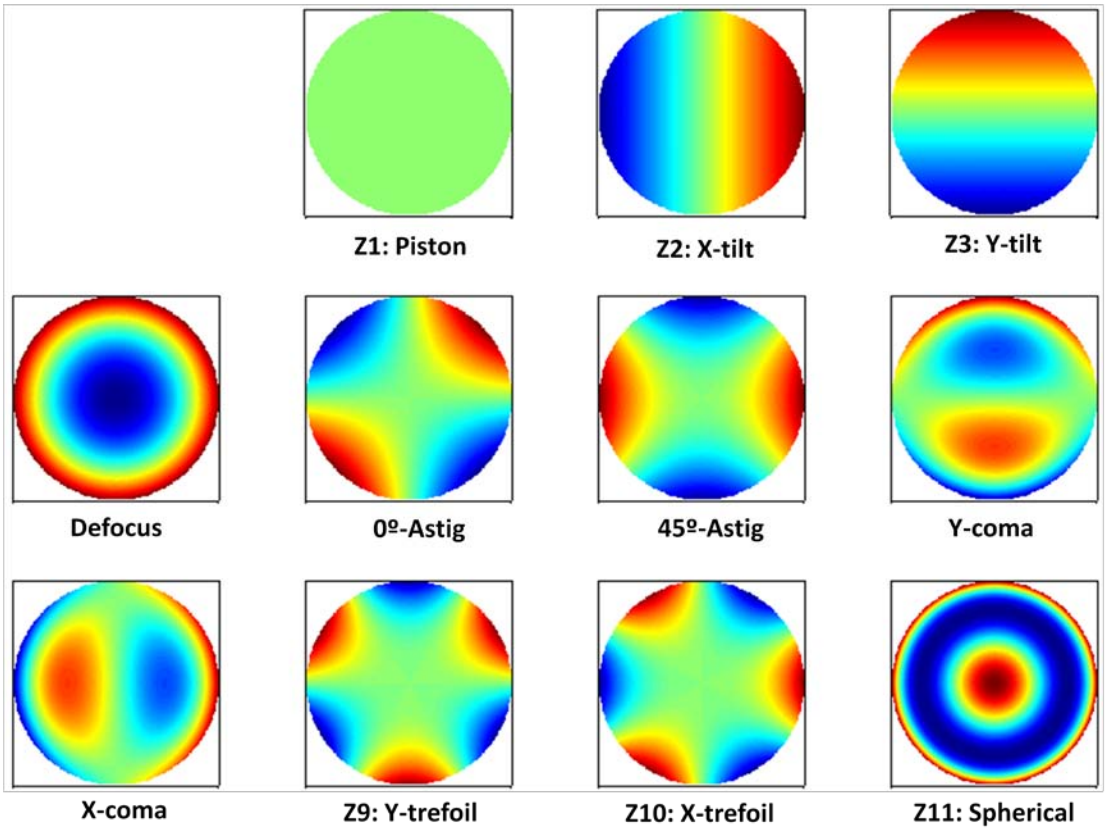

Figure 3: Zernike polynomial representation of an aberrated wavefront. The Zernike numbering system follows the Noll convention [4].

The DONUT program reconstructs the observed image intensity pattern based on the Zernike wavefront representation. Fig. 4 shows a stellar image (left panel) and the modeled intensity distribution generated by the Zernike reconstruction (right panel). The full analysis compares the Zernike coefficients for 25-40 individual stars per frame in order to sample multiple field points.

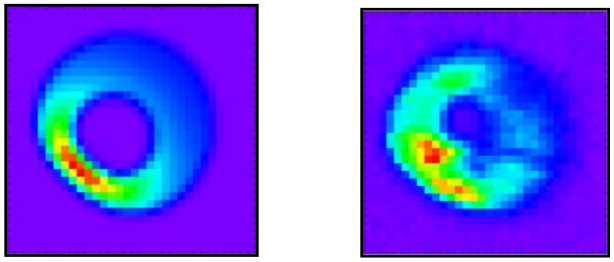

Figure 4: The observed (left) and modeled (right) fit to an individual stellar image. The modeled image passes a χ^2 goodness of fit test.

Conversion from the measured Zernike aberration coefficients to mirror motions is accomplished through the use of a Zemax model of SST. The Zemax model incorporates the imperfections of the actual delivered optical elements. It is useful to work with the as-built model instead of the ideal model in order to avoid confusing the effects of mirror misalignment with intrinsic aberrations due to surface deformities and mounting of the optics on the actuators. There remains, however, an ambiguity in the representation of the modeled mirror positions relative to

one another compared to their actual installed locations. This distinction manifests itself essentially as offsets to the zero points of the mirror positions.

By moving individual elements in simulation, we predict the sizes of aberrations. These predicted mirror motions-to-aberrations are collectively referred to as a sensitivity analysis. The Zemax sensitivity analysis provides a complicated set of relationships between mirror motions in each of the degrees of freedom and the resulting aberrations in the image [5]. But by choosing a limited set of motions, which dominate the aberrations – tertiary and secondary – we produce a tractable analysis between modeled and measured aberrations necessary in order to improve the SST spot size.

3. INITIAL FOCUS AND ALIGNMENT AT ZENITH

At first light in February 2011, the SST measured a spot size of 70 μm. Initial efforts at coarse focus and alignment brought the spot size down to 45μm. The initial efforts included adjustment of the CCD camera structure with respect to the primary mirror and alignment of the tertiary mirror cell within the structure.

After the preliminary focus activities, fine focus and alignment of the SST was accomplished using a 5-step iterative process to find the optimal mirror positions at a given temperature for the zenith pointing case.

1. *Focus by tertiary mirror piston:* The first step in the focus and alignment process is to minimize defocus aberration by translation of the tertiary mirror along the optical axis, i.e. "focusing" the telescope. The focus is performed by measuring the spot size for a series of tertiary mirror positions and fitting a quadratic to the curve of spot size as a function of mirror position. The minimum of the curve is the best focus position.
2. *Spherical aberration with secondary-plus-tertiary piston:* The second step is to reduce the spherical aberration by a coordinated translation of both the tertiary and secondary mirrors. The total path length remains constant as the two mirrors are translated in equal and opposite directions with respect to the optical axis. Keeping the path length constant leaves the defocus aberration unchanged. However, the magnitude of spherical aberration, which produces an increase in spot size that is uniform across the field of view, varies as a function of the coordinated mirror positions. We look for the "sweet spot" where both defocus and spherical aberration are simultaneously minimized. This procedure is unique to three-mirror telescopes.
3. *Measurement of higher order aberrations:* The third step in the alignment process is to acquire out of focus images by moving the tertiary mirror along the optical axis to produce "donuts". The DONUT software is used to estimate the Zernike aberrations in the system as described in Section 2. We acquire images on either side of focus for comparison and estimates of systematic errors (weather, hydraulic control, etc.).
4. *Identification of higher order aberrations:* Association of the Zernike aberration coefficients measured by DONUT with the Zemax sensitivity analysis leads to predictions for compensatory mirror motions.
5. *Application of mirror solutions:* In the fifth step, we apply the mirror alignment corrections, paying particular attention to coma and astigmatism, which are indicative of mirror tilts and offsets.

We repeat steps 1-5 to drive down the telescope spot size. The iterations continue until the spot size meets the system requirement. It is necessary to work on a night with excellent seeing conditions (sub-arcsec) and a stable temperature load on the telescope structure. We utilized DIMM systems as an independent measure of the seeing conditions where possible to separate the effects of seeing from those of alignment.

3.1. OPERATIONAL FINE FOCUS AND ALIGNMENT

Initial focus and alignment provided a starting point from which to develop the more complex dynamic models needed to control for elevation--induced gravity sag and temperature. This process also relied on analysis of using DONUT and the Zemax sensitivity analysis previously discussed. The effects of elevation and temperature are nominally considered independent to facilitate the development of predictive tertiary and secondary mirror position models within the SST telescope control software. We separately discuss each below. The combination of these two operational processes has reduced the overall SST spot size to as low as 28 μm rms diameter during optimal

seeing conditions. The model of the as-built system predicts a spot size of ~26 um, which does not account for the detector pixelization an therefore is an underestimate of expected performance.

3.2. MAINTAINING FOCUS AND ALIGNMENT UNDER GRAVITY SAG

Once the mirror alignment at zenith pointing reaches performance goals, the next step is to measure the aberrations introduced as a function of elevation angle. Even with extensive mirror support structures to maintain the position of mirrors in the cells, gravity tends to cause the mirror position to sag when pointed at low elevation. This is especially critical in a Mersenne-Schmidt telescope as *both* the tertiary mirror and secondary mirror sag relative to the primary. In a two-mirror telescope, the primary and secondary mirrors sag in the same direction, preserving to first order the orientation of the two. However, gravity sag causes the secondary and tertiary mirrors move in opposite directions with respect to the primary mirror. In practice, corrections are applied to the tertiary mirror. We first measure the defocus as a function of elevation angle by stepping the tertiary mirror position along the optical axis to find the minimum spot size, as described in the previous section, at several elevations. We find the defocus is well described by a quadratic line fit to the shift in tertiary mirror position as a function of elevation angle. After applying the correction to the tertiary fit, we then acquire a set of purposely defocused images for analysis with the DONUT program.

The most significant aberration that appears as a function of elevation angle is the Z7 term (y-coma). Our sensitivity analysis indicates that tilt about the elevation axis or decenter about the elevation axis of either the tertiary or secondary mirror introduce y-coma. The selection of which mirror motion model to apply was determined by considering other aberrations introduced into the system by the corrective mirror motions. We find the best results for overall aberration reduction and improved symmetry across the focal plane result from adjustment to the x-rotation of the tertiary mirror as a function of elevation angle. Figure 5 shows the performance of the elevation correction.

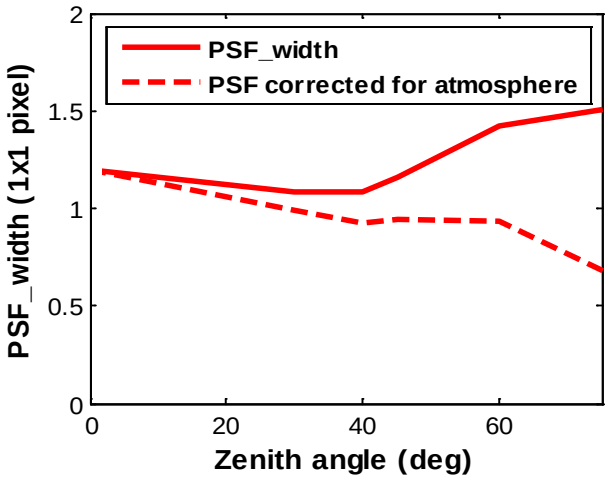

Figure 5: The performance of the elevation correction is demonstrated in the plot of spot size as a function of zenith angle. The data represent the mean value for all of the stars measured in each image at each elevation angle. The atmospheric correction assumes the standard model where the PSF increases proportional to (airmass)$^{0.6}$. The slight decrease in spot size at low elevation (large zenith angle) is due to a combination of improved alignment performance and overestimation of the atmospheric correction on a night with particularly good conditions.

3.3. VARIATION WITH TEMPERATURE

The steel telescope structure expands or contracts according to the ambient temperature. Over the course of a year, the nautical twilight temperature varies from a low of about -12º C in winter to a high of 25º C in summer. Environmental control of the telescope dome, designed by M3 Engineering, helps to regulate the temperature environment. Dome pre-conditioning is used primarily to prevent convection of the optics, which acclimate

relatively slowly. It also serves to minimize the temperature variation of the structure during the night by cooling the dome environment before the observing begins. Even with pre-conditioning, the structure temperature can still be expected to vary during the night.

We track the effect of temperature on the focus position with regular focus measurements in the manner described in Step 1 of Section 3.1. Over the course of the first year of operation, we build a temperature model for the SST:

$$TMz - SMz = C_1 * T_{avg} + C_2,$$

where *TMz* and *SMz* are the tertiary mirror and secondary mirror position along the optical axis, respectively. The average temperature of the telescope structure is T_{avg}, and the linear coefficients of best fit are C_1 and C_2. The empirical model between mirror position and temperature uses the average of the 58 temperature sensors on the telescope structure. In theory, the mirror position should be most sensitive to the temperature of the struts supporting the mirror cells, which determines the thermal expansion of the component associated with the mirror placement along the optical axis. We experimented with using the sensors on the mirror struts to build a temperature model, but found that the resulting line fit was adversely affected by the noisier temperature measurement. Because the telescope structure is nearly isothermal, taking the average over all temperature sensors on the structure reduces the uncertainty in the temperature reading, an advantage that outweighs the benefit of using more targeted temperature readings.

In practice, we adjust *TMz* to focus the telescope, i.e. to minimize the defocus aberration. The location of *SMz* is selected to minimize spherical aberration as described in Step 2 of Section 3.1, and its position also varies with the telescope structure temperature. We find that the model predicts the focus position to within 25 µm of travel of the tertiary mirror at each temperature point when the system is in thermal equilibrium.

4. SUMMARY AND CONCLUSION

We achieved focus and alignment of the three-mirror Mersenne-Schmidt type SST, a unique telescope system that has no predecessor or precedent for focusing methodology. Focus and alignment relied solely on measurements of optical aberrations observed in the imagery itself on a system that does not include a dedicated wavefront sensor.

The SST maintains a consistent spot size performance over a range of temperature and elevation conditions during a night's observing. The temperature model predicts the best focus position to within 25 µm (tertiary mirror location along the optical axis) when the system is in thermal equilibrium and is used to keep the telescope in focus as the ambient temperature varies over the course of a night. The elevation model successfully maintains in real-time the focus and alignment from zenith to horizon through the application of tertiary mirror adjustments.

The focus and alignment program for the SST has successfully brought the spot size down to 28 µm rms diameter during optimal seeing conditions. The minimum spot size compares favorably with the system performance prediction of 26 µm based on the Zemax model for the as-built optical system.

5. REFERENCES

1. Tokovinin A. and Heathcote S. *Donut: measuring optical aberrations from a single extra-focal image.* PASP, V. 118, pp. 1165-1175, 2006.
2. Roddier, F., *Wavefront Sensing and the Irradiance Transport Equation*, Appl. Opt., 29, 1402, 1990.
3. Kim, C.-J. and Shannon, R. R. *Catalog of Zernike Polynomials*, Appl. Optics and Optical Engineering, X, Chapter 4, Academic Press, 1987.
4. Noll, R. J. *Zernike polynomials and atmospheric turbulence*, JOSA, 66, 207, 1976.
5. Woods, D. F., Shah, R., Johnson, J., Szabo, A., Pearce, E. C., Lambour, R. Faccenda, W. *Focus and Alignment of a Three Mirror Mersenne-Schmidt Telescope*, in preparation